An Inner-spherical Continuously Variable Transmission for Electric Bicycles

Moon-Woo Park¹, Hyoung-Woo Lee²,# and No-Gill Park²

1 Department of Mechanical Design Engineering, Graduate School, Pusan National University, Jangjeon 2(i)-Dong, Geumjeong-Gu, Busan, South Korea, 609-735
2 School of Mechanical Engineering, Pusan National University, Jangjeon 2(i)-Dong, Geumjeong-Gu, Busan, South Korea, 609-735
Corresponding Author / E-mail: leehwoo@pusan.ac.kr, TEL: +82-51-510-2598, FAX: +82-51-582-9164

A new continuously variable transmission (CVT) for electric bicycles was developed using a traction drive mechanism with inner and outer spherical rotors. This electric bicycle CVT permits three propulsion modes: human-power only, motor-power only, or a combination of motor power and human power. In addition, the electric bicycle CVT has high power efficiency, large torque capacity, improved drivability, and good packageability. A prototype was manufactured based on a conceptual design, a performance analysis, and a detailed design. This prototype has a rated power of 250 W and input motor speed of 20 rad/s for an overall speed ratio in the range 0.3–1.2. A bench test was conducted to measure the power transmission performance of the prototype.

NOMENCLATURE

η = power efficiency of the ISCVT traction drive
ω_1, ω_2 = speed of the driving and driven rotors
T_1, T_2 = torque of the driving and driven rotors
r_1, r_2, r_c = radii of the driving, driven, and counter rotors
h = installed height of the bearing pedestal on the frame
ϕ = tilt angle of the rotating axis of the counter rotor
θ = contact angle between the driving/driven and counter rotors
δ = speed ratio of the ISCVT
N_1 = normal force on the contact area between the driving and counter rotors
$\mathbf{r}_1$, $\mathbf{r}_2$ = radius vectors of the driving and driven rotors
$\boldsymbol{\rho}_1$, $\boldsymbol{\rho}_2$ = local position vectors of the contact areas between the driving/driven and counter rotors
$\boldsymbol{\tau}_1$, $\boldsymbol{\tau}_2$ = shear pressure vectors of the contact areas between the driving/driven and counter rotors

1. Introduction

An electric bicycle is a general purpose bicycle with an electric motor powered by a battery or a fuel cell. For best performance, an electric bicycle needs a transmission that handles three propulsion modes, human-power only, motor-power only, and motor power plus human power, but most electric bicycles do not have this feature. The common electric bicycle transmission suffers from poor convenience and drivability due to separated drivelines for human power and motor power.[1] To improve both convenience and drivability of the transmission, research and development efforts have concentrated on methods using chain sprockets and/or gears, but the resulting

transmissions are complicated and heavy.[2]

Since the requirement is for a simple and compact transmission that provides convenience and drivability, continuously variable transmissions (CVT) would appear to be a promising avenue of research.[3]

In this study, we apply a new inner-spherical CVT (ISCVT) design to an electric bicycle transmission. This has a traction drive transmitting power through contacts between inner and outer spheres. The ISCVT has been shown to be quite practical on bicycles, scooters, and automotive transmissions.[3-6] The ISCVT for a bicycle[3] has a friction drive mechanism, a four-bar linkage ratio changer, and bolt-fastened pressure device. An ISCVT on an electric bicycle would be suitable from the viewpoints of efficiency, power capacity, and packageability. The new ISCVT in this paper has a traction drive mechanism, a simple ratio changer, and a spring pressure device, which are improvements over the conventional design. After conducting a conceptual design, a performance analysis, and a detailed design, we manufactured a prototype of the ISCVT for an electric bicycle. This prototype had a rated power of 250 W, a speed of 20 rad/s, and an overall speed ratio range of 0.3 to 1.2. We conducted a bench test to evaluate the power transmission performance of this prototype.

2. ISCVT for the Electric Bicycle

2.1 Mechanism Layout

Figure 1 shows the driveline of the electric bicycle CVT consisting of the ISCVT assembly, belt pulleys, and an electric motor. The ISCVT is installed on the side of the rear wheel and attached directly to the rear axle. The belt pulleys connecting the pedals to the ISCVT drive shaft are configured with a fixed gear ratio, and a one-way clutch is used in the inner race of the rear pulley.
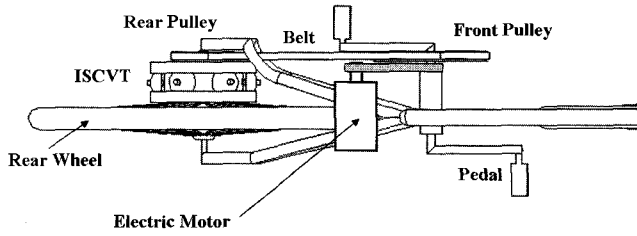
Fig. 1 Driveline of the electric bicycle CVT

The electric motor is also connected to the pedal shaft belt pulleys. Chain sprockets could be used instead of belt pulleys without affecting the drivability.

2.2 Features of the ISCVT

Figure 2 shows a sectional view of the ISCVT assembly on the rear wheel hub. The ISCVT assembly consists of the traction drive variator, pressure device, and ratio changer. The traction drive variator consists of the driving-, the driven-, and six counter-rotors with inner and outer spherical surfaces.
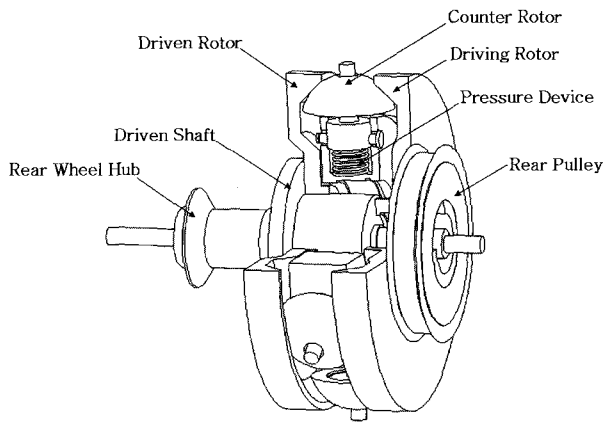

Fig. 2 ISCVT assembly

Transmission of power is possible due to the high shear resistance of the lubricant existing as a thin oil film between the rolling contact areas of the rotors. This type of lubrication is known as elasto-hydrodynamic lubrication, which transmits power through the thin oil film and keeps the CVT going for long time.[7] Because the inner and outer spherical contacts of the ISCVT reduce stress on the rolling contact areas, the fatigue life is increased and the torque capacity is maximized in comparison with the Toroidal, Kopp-Ball, Milner, or disk types of CVT. In addition, the power efficiency is superior because the inner and outer circular spherical contacts reduce spin loss.[3-6]

The power efficiency of the ISCVT traction drive is given by

$$\eta = \frac{\omega_2 T_2}{\omega_1 T_1} \qquad (1)$$

where the unknown variables ω_2 (speed of the driven rotor) and T_2 (torque of the driven rotor) are determined from the equilibrium equations for axial torque, which apply to the two rolling contact areas of the rotors considering the traction coefficients of the SANTOTRAC-50 lubricant. Variables ω_2 and T_2 are calculated from Eqs. (2-2), (2-3), and (2-4):[3]

$$\int_{A_1} (\mathbf{r}_1 + \mathbf{\rho}_1) \times \mathbf{\tau}_1 dA_1 - T_1 = 0 , \qquad (2)$$

$$\int_{A_1} (\mathbf{r}_1 + \mathbf{\rho}_1 - \mathbf{a}_1) \times \mathbf{\tau}_1 dA_1 + \int_{A_2} (\mathbf{r}_2 + \mathbf{\rho}_2 - \mathbf{a}_2) \times \mathbf{\tau}_2 dA_2 = 0 , \text{ and} \qquad (3)$$

$$\int_{A_2} (\mathbf{r}_2 + \mathbf{\rho}_2) \times \mathbf{\tau}_2 dA_2 - T_2 = 0 \qquad (4)$$
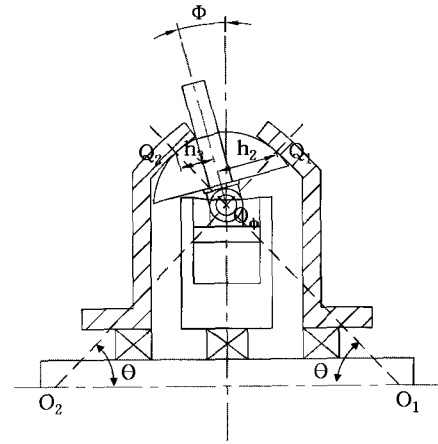

Fig. 3 Kinematic diagram of the ISCVT

The contact stress of the rolling contact areas is calculated using the Hertz contact theory[8] and the fatigue life is determined from an equation based on the Lundberg-Palmgren theory.[9]

The ISCVT changes speed continuously by altering the tilt angle of the rotating axis of each counter rotor between the driving and driven rotors. The speed ratio of the ISCVT is defined as the driven rotor speed versus the driving rotor speed. Referring to Fig. 3, the speed ratio is the ratio of the radii (h_2, h_3) of the contact points (Q_1, Q_2) of the rotating axis tilted at an angle of ϕ, as follows:

$$\delta = h_3 / h_2 \qquad (5)$$

where

$$h_2 = r_c \sin(\theta + \phi) \quad \text{and} \qquad (6)$$

$$h_3 = r_c \sin(\theta - \phi) \qquad (7)$$

3. Conceptual Design

To verify the practicality of the proposed ISCVT for an electric bicycle, we chose the design specifications listed in Table 1 and conducted a conceptual design. Figure 4 shows the design procedure we used to obtain feasible solutions for satisfying the design constraints summarized in Table 2. The design variables considered in the optimization process included the radii (r_1, r_2, r_c) of inner and outer spheres on the driving, driven, and counter rotors, respectively; the installed height (h) of the bearing pedestal on the frame; and the cam inclination angles (λ) of the pressure devices. The best solution is a feasible solution with maximum efficiency. The design results are listed in Table 3. The overall diameter and width are $\Phi 210$ mm and 74 mm, respectively.

Table 1 Design Specifications

Parameters	Motor-powered	Human-powered
Rated power (P_i)	250 W	100 W
Rated input speed (Ω_i)	20 rad/s	6 rad/s
Overall speed ratio (δ)	0.3–1.2	1.0–4.0
Sprocket gear ratio	0.6	2.0

Table 2 Design Constraints

	r_1, r_2	$r_1 = r_2 \leq 150$ mm
Variable constraints	r_c	$r_c \leq 35$ mm
	h	$60 \leq h \leq 80$ mm
Installation constraints	Overall size limit	$\Phi\ 220 \times 120$ mm
Performance constraints	Efficiency limit	85 %
	shear stress limit	500 Mpa
	Fatigue life	1 Gh

Table 3 Design Results

Variables		Performance	
r_1, r_2	121.43 mm	Efficiency	92%
r_c	28.54 mm	Shear stress	298.4 MPa
H	70.35 mm	Fatigue life	10 Gh
Spring force	856 N	Overall size	Φ 210 × 74 mm

Fig. 4 Flowchart of the design process

Fig. 5 Average efficiency in the whole range of speed ratios

For the best solution in case of motor-power, Fig. 5 shows simulated results of the average efficiency as a function of the variable input speed over the whole range of speed ratios. The variation of the efficiency is very slight, and is consistent near 90% efficiency. For the rated power, the maximum shear stress acting on the contact area between the spherical rotors is 298.4 MPa. Theoretically estimated fatigue life is calculated as 10 Gh, based on the Lundberg–Palmgren theory.

4. Prototype Evaluation

4.1 Prototype Manufacturing

Based on the results of the optimal design listed in Table 3, we carried out a detailed design to determine bearing selections and dimensions of the mechanism elements. We constructed a solid model prototype with commercial CAD software (shown in Fig. 6). We chose chromium–molybdenum alloy steel (AISI4140)[10] for the material. The manufactured prototype is shown in Fig. 7.
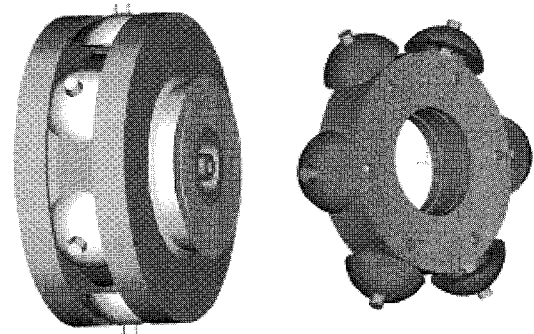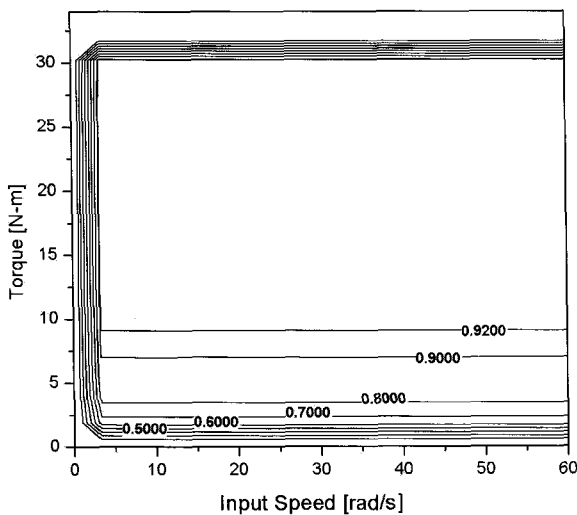

Fig. 6 A solid model of the ISCVT prototype

Fig. 7 The manufactured ISCVT prototype

4.2 Prototype Bench Test

Figure 8 presents a schematic diagram and Fig. 9 shows a photograph of the test rig used to measure the ISCVT power transmission efficiency. The test rig consisted of a power source (AC servomotor), torque sensor, photo sensor, and dynamometer. The ISCVT drive shaft is connected to the torque sensor by a timing belt and pulleys with a fixed ratio of 1:1, and the driven shaft is directly connected to the dynamometer. The test conditions are listed in Table 4. The measured efficiencies of the test are shown in Figs. 10–12. The difference between the calculated efficiency shown in Fig. 5 and the measured efficiency shown in Figs 10–12 is about 10–20%. This difference is due to a manufacturing error in the rotors, bearing loss, and unstable lubricant conditions. However, the trends between the measured and calculated results are similar.
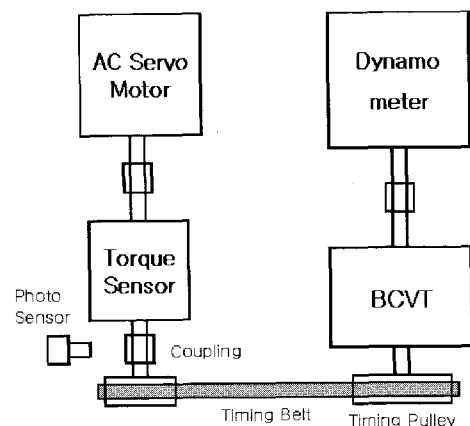

Fig. 8 Schematic diagram of the ISCVT test rig

Figures 10–12 show that the maximum measured power efficiency is 84.9% for an overall speed ratio of 0.3. The power efficiency decreases as the speed ratio increases. However, the variation in measured efficiency is very slight, and it is consistent as the input speed changes. Thus the transmission is suitable for an electric bicycle with different types of power input sources (e.g., motor power and human power).
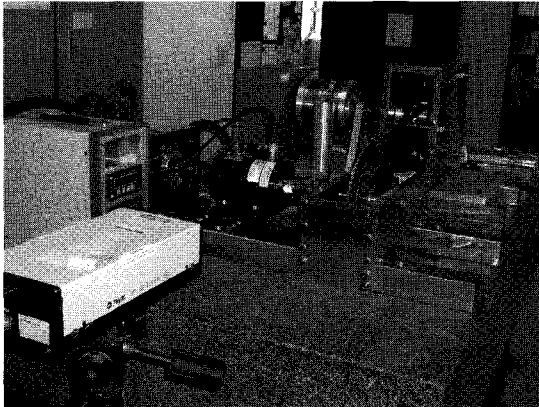

Fig. 9 Photograph of the ISCVT test rig

Table 4 Test conditions

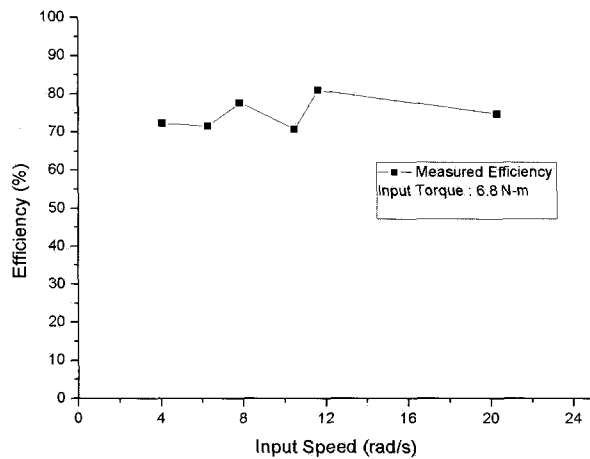| Overall speed ratio	0.3, 0.6, 1.2
Input speed (rad/s)	4, 6, 8, 10, 12, 20, 30, 40, 50, 60
Input torque (N-m)	6.8, 7.7, 8.0 with output shaft loaded by dynamometer

Fig. 10 Efficiency measured during the bench test for an overall speed ratio of 0.3
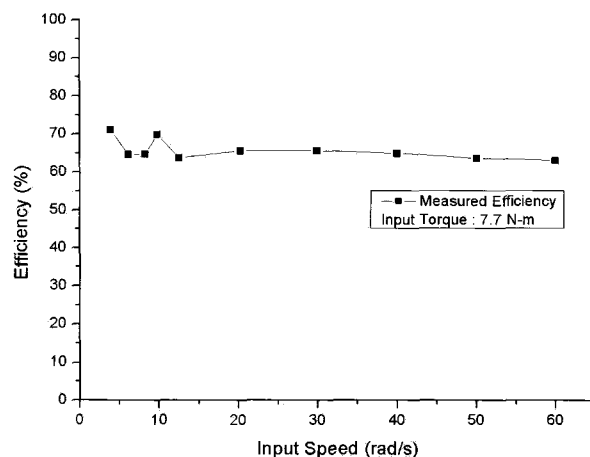

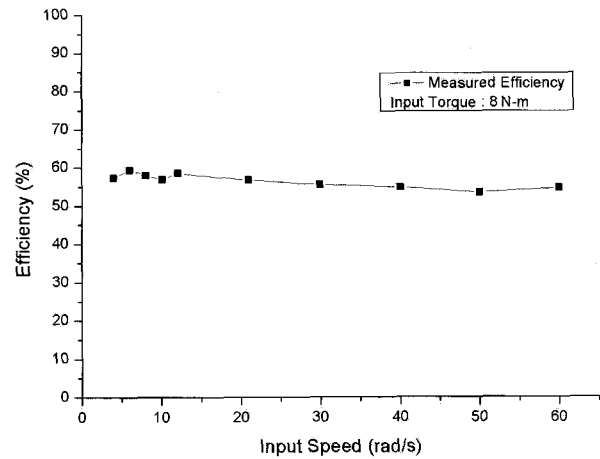Fig. 11 Efficiency measured during the bench test for an overall speed ratio of 0.6

Fig. 12 Efficiency measured during the bench test for an overall speed ratio of 1.2

5. Conclusion

The new ISCVT was designed for electric bicycles to improve both convenience and drivability of the transmission. A prototype was built based on the optimal design process that considered the various constraints on the efficiency, stress, fatigue life, and dimensions. A bench test of this prototype was conducted to measure its power transmission performance. The results are as follows.

(1) An overall diameter of $\Phi210$ mm and width of 74 mm are possible.
(2) The maximum power efficiency is 84.9%, measured at an overall speed ratio of 0.3.
(3) Variations in the measured efficiency are very small, and consistent as the input speed changes, so that the transmission is suitable for an electric bicycle with various sources of input power.
(4) Commercial production of this prototype is a possibility.

REFERENCES

1. Lomonova, E. A., Vandenput, A. J. A., Rubacek, J., d'Herripon, B. and Roovers, G., "Development of an Improved Electrically Assisted Bicycle," Industry Applications Conference, Vol. 1, pp. 384-389, 2002.

2. Andreassi, L., Cordiner, S. and Romanelli, F., "Conceptual Design and Modeling of a Fuel Cell Pedal Assisted Bicycle," SAE, Technical Paper No. 2004-32-0049, 2004.

3. Seong, S. H., Ryu, J. H. and Park, N. G., "Conceptual Design of Inner-Spherical Continuously Variable Transmission for Bicycle Usage," International Journal of Automotive Technology, Vol. 6, No. 5, pp. 467-473, 2005.

4. Ryu, J. H., Kim, J. H. and Park, N. G., "Development of the Inner Spherical Traction CVT for Scooters," Fall Conf. Proc. of KSAE, pp. 577–581, 2004.

5. Ku, I. K. and Park, N. G., "An Introduction of a New Traction Drive Pairing with the Inner and the Outer Surface of the Spherical Rotors for Automobile Usage," International Continuously Variable and Hybrid Transmission Congress, 2004.

6. Park, M. W., Lee, H. W., Park, N. G and Sang H. S., "Development of Inner-Spherical Continuously Variable Transmission for Bicycles," International Journal of Automotive Technology, Vol.8, No.5, pp. 593-598. 2007.

7. Heilich, F. W. and Shube, E. E., "Traction Drives: Selection and Application," Marcel Dekker, pp. 234-320, 1983.

8. Pillkey, W. D., "Formulas for Stress, Strain and Structural Matrices," John Wiley, pp. 514-550, 1994.

9. Rohn, D. A., Loewenthal, S. H. and Coy, J. J., "Simplified Fatigue Life Analysis for Traction Drive Contacts," ASME Journal of Mechanical Design, Vol. 103, No. 1, pp. 430-439, 1981.

10. Harvey, P. D., "Engineering Properties of Steel," American Society for Metals 2nd edn. Metals Park, pp. 134-150, 1999.